A COVID-19 mathematical model of at-risk populations with non-pharmaceutical preventive measures

The case of Brazil and South Africa

Asempapa, Reuben; Oduro, Bismark; Apenteng, Ofosuhene O.; Magagula, Vusi M.

Published in:
Infectious Disease Modelling

Link to article, DOI:
10.1016/j.idm.2021.11.005

Publication date:
2022

Document Version
Publisher's PDF, also known as Version of record

Infectious Disease Modelling 7 (2022) 45–61

Contents lists available at ScienceDirect

Infectious Disease Modelling

journal homepage: www.keaipublishing.com/idm

A COVID-19 mathematical model of at-risk populations with non-pharmaceutical preventive measures: The case of Brazil and South Africa

Reuben Asempapa [a], Bismark Oduro [b], Ofosuhene O. Apenteng [c], Vusi M. Magagula [d, *]

[a] School of Behavioral Sciences and Education, Penn State University, Middletown, PA, 17 057, USA
[b] Department of Mathematics and Physical Sciences, California University of Pennsylvania, California, PA, 15 419, USA
[c] Research Group for Genomic Epidemiology, National Food Institute, Technical University of Denmark, Kemitorvet, 2800, Kgs. Lyngby, Denmark
[d] Faculty of Science and Engineering, Department of Mathematics, University of Eswatini, Private Bag 4 Kwaluseni, Matsapha, Eswatini

ARTICLE INFO

Article history:
Received 25 October 2020
Received in revised form 23 November 2021
Accepted 24 November 2021
Available online 1 December 2021
Handling editor: Dr Y. Shao

Keywords:
COVID-19 disease
Low-risk population
High-population
Effective reproduction number
Preventive measures

ABSTRACT

This work examines a mathematical model of COVID-19 among two subgroups: low-risk and high-risk populations with two preventive measures; non-pharmaceutical interventions including wearing masks, maintaining social distance, and washing hands regularly by the low-risk group. In addition to the interventions mentioned above, high-risk individuals must take extra precaution measures, including telework, avoiding social gathering or public places, etc. to reduce the transmission. Those with underlying chronic diseases and the elderly (ages 60 and above) were classified as high-risk individuals and the rest as low-risk individuals. The parameter values used in this study were estimated using the available data from the Johns Hopkins University on COVID-19 for Brazil and South Africa. We evaluated the effective reproduction number for the two countries and observed how the various parameters affected the effective reproduction number. We also performed numerical simulations and analysis of the model. Susceptible and infectious populations for both low-risk and high-risk individuals were studied in detail. Results were displayed in both graphical and table forms to show the dynamics of each country being studied. We observed that non-pharmaceutical interventions by high-risk individuals significantly reduce infections among only high-risk individuals. In contrast, non-pharmaceutical interventions by low-risk individuals have a significant reduction in infections in both subgroups. Therefore, low-risk individuals' preventive actions have a considerable effect on reducing infections, even among high-risk individuals.

* Corresponding author.
E-mail addresses: rsa26@psu.edu (R. Asempapa), oduro@calu.edu, biskodo@gmail.com (B. Oduro), ofap@food.dtu.dk (O.O. Apenteng), gutjwa@gmail.com, vmmagula@uniswa.sz (V.M. Magagula).

Peer review under responsibility of KeAi Communications Co., Ltd.

https://doi.org/10.1016/j.idm.2021.11.005

1. Introduction

A novel coronavirus emerged in December 2019 in Wuhan, China, which attracted the attention of both the Chinese government and the international community. The potential causes of this novel coronavirus were omitted, including influenza, avian influenza, adenovirus, severe acute respiratory syndrome coronavirus (SARS-CoV), and Middle East respiratory syndrome coronavirus (MERS-CoV). However, most epidemiologists and scientists suggested that the case infection of the novel virus was related to the South China seafood. By January 7, 2020, the causative pathogen for the novel virus was identified as a new coronavirus (2019-nCoV), followed by gene sequence analysis and the development of detection methods (Guan et al., 2020; Huang et al., 2020; Li et al., 2020; Wang et al., 2020a; World Health Organization, 2020; Zhu et al., 2020). The World Health Organization (WHO) officially named the novel virus the severe acute respiratory syndrome coronavirus 2 (SARS-CoV-2) (Zheng et al., 2020). The novel coronavirus is a pathogen that targets the human respiratory system and is mostly referred to as COVID-19. Since the infectious disease (COVID-19) was first identified, it has spread to more than 200 countries globally, resulting in the 2020 global pandemic. Compared to other coronaviruses, the number of deaths attributed to COVID-19 significantly exceeds the other two coronaviruses (SARS-CoV and MERS-CoV).

As of the time of writing this article, the global outbreak caused by COVID-19 continues. The explosive nature and associated high mortality of the epidemic pose a considerable threat to global public health and the economy (World Health Organization, 2020)(WHO, 2020; CDC, 2020). To contain the spread of the COVID-19, the WHO suggested that certain measures need to be taken to control the spread of COVID-19 including, frequent washing of hands with soap, maintaining social distancing of at least six-feet, wearing masks in public places, effective mass testing, and possibly locking places down where the infection rates are incredibly high. Few countries have managed to bring down many of their cases in a short period due to their mitigation strategies and risk assessments (Anderson, Heesterbeek, Klinkenberg, & Hollingsworth, 2020; Onder et al., 2020). The COVID-19 virus has caused a lot of damage economically, health-wise, and otherwise. It has been shown that patients with underlying health conditions (Chen et al., 2020) are more likely to die from the virus and the elderly (Wang et al., 2020b) as well. Wang et al.(Wang et al., 2020b) noted that the virus is highly fatal and progresses rapidly in individuals with comorbidities and above 60 years of age. In this study, we classify these groups as high-risk and all others as low risk. A study by Chen et al.(Oduro and Magagula, 2021) showed that deceased patients' median age was significantly older than recovered patients and that chronic hypertension and other cardiovascular comorbidities were more frequent among deceased patients than recovered patients. Additionally, Wang et al. (Wang et al., 2020b) stated that a high proportion of severe to critical cases and high fatality rates were observed in the elderly COVID-19 patients. Their study also suggested that COVID-19 rapidly progressed in the elderly with a median survival time of five days after admission. The fatality was also very high with dyspnea, lymphocytopenia, comorbidities, cardiovascular disease and chronic obstructive pulmonary disease, and acute respiratory distress syndrome. Therefore, these studies suggest that COVID-19 in elderly patients is severe and highly fatal and can progress rapidly in those with comorbidities.

Additionally, Kobayashi et al. (Kobayashi et al., 2020) observed that the risk of death associated with COVID-19 among young adults was higher than seasonal influenza, and the elderly with underlying comorbidities require optimal care. Moreover, Martins-Chaves et al.(Martins-Chaves, Gomes, & Gomez, 2020) explained that the elderly, males, hypertensive, patients with comorbidities, constitute the most well-characterized high-risk group for severe manifestations from COVID-19. It is crucial to understand the dynamics of the interactions between those at low-risk and those at high-risk. Understanding these dynamics will enhance preventative measures of infections and reduce the number of cases and probably the number of deaths. Quantifying the interactions' dynamics requires some mathematical models, which has the potential to enhance our understanding of the parameters associated with the increase in infection rates. Researchers who study and describe infectious diseases' behaviors have increasingly relied on mathematical models for their work (Diekmann, Heesterbeek, & Britton, 2012; Heesterbeek, 2002; Mishra, Fisman, & Boily, 2011). Additionally, some researchers have formulated and used several mathematical models to examine and understand the dynamics of COVID-19 in different situations (Bai et al., 2020; Jewell, Lewnard, & Jewell, 2020; Ndairou, Area, Nieto, & Torres, 2020, p. 109846; Oduro and Magagula, 2021). Our aim here is to present a mathematical model to understand the dynamics of the interactions between people who are at low-risk and those at high-risk. The model was fitted to data obtained from the Johns Hopkins University (Johns Hopkins University., 2020) for Brazil and South Africa. In the next section, we present the mathematical model used in this study with a detailed description of the solution approach based on the Runge-Kutta method built-in MATLAB. The rest of the article was organized as follows: In section 2, we formulate and describe the model in detail, section 3 addresses and describes the effective reproduction number, the model analysis with the results, and discussion are presented in sections 4. Finally, we summarize and conclude our work with recommendations in section 5.

2. Model formulation

In this section, we present the mathematical model that will enhance our understanding of the dynamics of the interactions between those who are at low-risk and those who are high-risk. Our model was divided into eight compartments namely, high-risk Susceptible (S_h), low-risk Susceptible (S_l), high-risk Exposed E_h, low-risk Exposed (E_l), high-risk Infected (I_h), low-risk Infected (I_l), Hospital (H), and Recovered populations, respectively (R). The main assumption was that all constants are positive. We assumed that the high-risk susceptible population become exposed after interacting with the high-risk infected, low-risk infected populations, and with those who are hospitalized. Similarly, those who are low-risk susceptible

population become exposed after interacting with the high-risk infected, low-risk infected populations, and with those who are hospitalized. We introduce a modification parameter v to account for the variability in the spread of the infection by hospitalized individuals, in comparison to other infectious classes. The transmission rate β_l is reduced by non-pharmaceutical interventions including wearing masks, maintaining social distance, and washing hands regularly at the proportion ϵ_l.

In addition to the interventions listed above, high-risk individuals must take extra precaution measures, including telework, avoiding social gathering or public places, etc. to reduce the transmission β_h by ϵ_h. This implies that $0 < \epsilon_l \leq \epsilon_h < 1$. The exposed population (both high-risk and low-risk) progress to the infectious classes at the rate k_h and k_l, respectively. Infected individuals (both high-risk and low-risk) can either be hospitalized or recover at the rate σ_h and σ_l, respectively. The fraction of those that get hospitalized is denoted by ρ_h and ρ_l from the high-risk infectious class and low-risk infectious class, respectively. The hospitalized recover at the rate α. The infectious individuals die due to the disease at the rate δ_h and δ_l, respectively, for high-risk and low-risk. We denote the disease-induced mortality rate for the hospitalized individuals by δ. The dynamics model is displayed in Fig. 1 below, and the descriptions of the variables are presented in Table 1 and 2.

The dynamics in Fig. 1 can be represented as a system of nonlinear ordinary differential equations given by

$$\begin{aligned}
\frac{dS_l}{dt} &= -\beta_l(1-\epsilon_l)(I_h + I_l + vH)\frac{S_l}{N} \\
\frac{dE_l}{dt} &= \beta_l(1-\epsilon_l)(I_h + I_l + vH)\frac{S_l}{N} - k_l E_l \\
\frac{dI_l}{dt} &= k_l E_l - (\sigma_l + \delta_l) I_l \\
\frac{dS_h}{dt} &= -\beta_h(1-\epsilon_h)(I_l + I_h + vH)\frac{S_h}{N} \\
\frac{dE_h}{dt} &= \beta_h(1-\epsilon_h)(I_l + I_h + vH)\frac{S_h}{N} - k_h E_h \\
\frac{dI_h}{dt} &= k_h E_h - (\sigma_h + \delta_h) I_h \\
\frac{dH}{dt} &= \rho_h \sigma_h I_h + \sigma_l \rho_l I_l - \alpha H \\
\frac{dR}{dt} &= (1-\rho_h)\sigma_h I_h + (1-\rho_l)\sigma_l I_l + \alpha H.
\end{aligned} \tag{1}$$

The COVID-free equilibrium ($\varkappa_o$) of the model (1) is given by

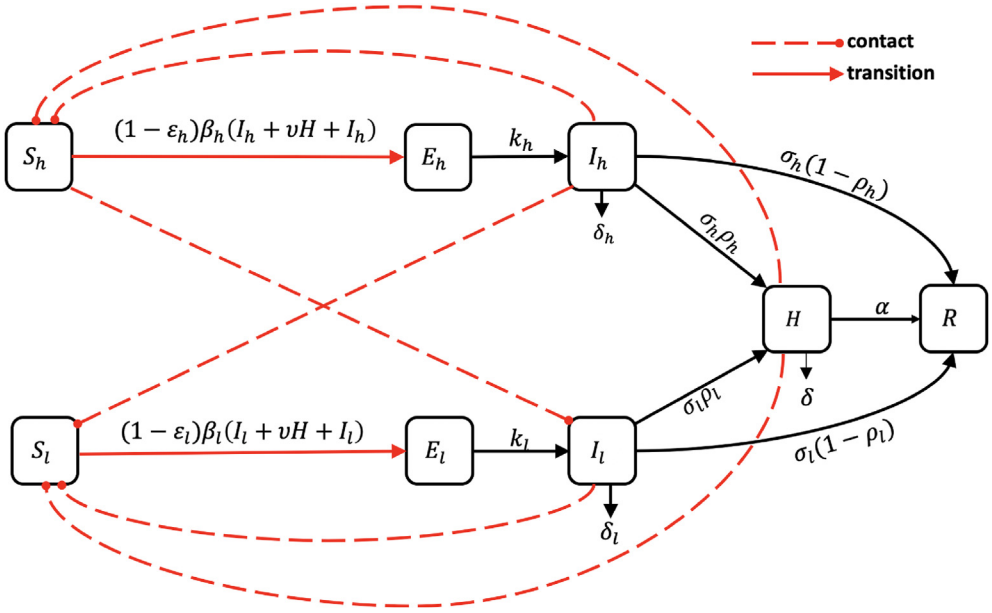

Fig. 1. Schematic diagram of the COVID-19 model.

Table 1
Description of state variables of the COVID-19 model.

State variable	Description
S_h	Population of high-risk susceptible individuals
S_l	Population of low-risk susceptible individuals
E_h	Population of high-risk early-exposed individuals (i.e., newly-infected individuals who are not yet infectious)
E_l	Population of low-risk early-exposed individuals (i.e., newly-infected individuals who are not yet infectious)
I_h	Population of high-risk infectious individuals
I_l	Population of low-risk infectious individuals
H	Population of hospitalized individuals
R	Population of recovered individuals

Table 2
Description of the parameters of the COVID-19 model (1).

Parameter	Description
β_l	Effective community contact rate of low-risk
β_h	Effective community contact rate of high-risk
ν	Modification parameter
ϵ_l	Non-pharmaceutical intervention by low-risk to reduce the transmission.
ϵ_h	Non-pharmaceutical intervention by high-risk to reduce the transmission.
$k_l = k_h$	Rate of progression from exposed class to infected classes ($\frac{1}{k_l} = \frac{1}{k_h}$ is the latent period)
$\sigma_l\rho_l$	Rate of progression from infected low-risk (I_l) to hospitalized class (H)
$\sigma_h\rho_h$	Rate of progression from infected high-risk (I_h) to hospitalized class (H)
$\sigma_l(1-\rho_l)$	Rate of progression from infected low-risk (I_l) to recovery class (R)
$\sigma_h(1-\rho_h)$	Rate of progression from infected high-risk (I_h) to recovery class (R)
α	Recovery rate for individuals from H class to R
δ_l	Disease-induced mortality rate for infectious individuals of low-risk
δ_h	Disease-induced mortality rate for infectious individuals of high-risk
δ	Disease-induced mortality rate for hospitalized individuals

Table 3
Parameters of the model (1).

Parameter	Default values	Reference
$k_l = k_h$	1/4 day^{-1}	(Li et al., 2020, Ngonghala et al., 2020, Ferguson et al., 2020)
$\sigma_l\rho_l$	1/7 day^{-1}	(Tang et al., 2020; Zhou et al., 2020)
$\sigma_h\rho_h$	1/7 day^{-1}	(Tang et al., 2020; Zhou et al., 2020)
ρ_h	0.25 day^{-1}	(Ferguson et al., 2020; Ngonghala et al., 2020)
α	1/14 day^{-1}	(Tang et al., 2020; Zhou et al., 2020)
δ	0.046day^{-1}	(Ferguson et al., 2020; Ngonghala et al., 2020)
δ_s	0.01 day^{-1}	(Ferguson et al., 2020; Ngonghala et al., 2020)
δ_h	0.02 day^{-1}	(Ferguson et al., 2020; Ngonghala et al., 2020)

Table 4
Fitted parameters of the model (1).

Country	β_l	β_h	ϵ_l	ϵ_h	V	$\mathcal{R}_l$	$\mathcal{R}_h$	$\mathcal{R}_0$
Brazil	0.930 6	0.336 1	0.272 9	0.343 2	0.131 6	1.255 4	0.146 3	1.401 7
South Africa	0.679 3	0.512 4	0.275 7	0.452 1	0.412 0	1.318 9	0.268 8	1.587 7

$$\varkappa_o = (S_l^*, E_l^*, I_l^*, S_h^*, E_h^*, I_h^*, H^*, R^*) = (S_l(0), 0, 0, S_h(0), 0, 0, 0, 0), \tag{2}$$

where $S_l(0)$ and $S_h(0)$ are the initial size of the susceptible individuals in low and high-risk sub-populations respectively. Note also that $S_l(0) + S_h(0) = N(0)$.

3. The effective reproduction number

One of the issues most discussed concerning COVID-19 is the effective reproduction number denoted by $\mathcal{R}_0$. It is the average number of secondary cases from a single infected individual. Additionally, the reproduction number offers a criterion that plays a vital role in determining whether the disease of the patient persists or dies out. According to Delamater et al. (2019), $\mathcal{R}_0$ is the mean indicator of secondary infections produced in a population where anyone can be infected, and it is used

to calculate the risk for transmission of a communicable disease like COVID-19. Similarly, $\mathcal{R}_0$ can be defined as the reproduction number when no immunity from past exposures has occurred. For $\mathcal{R}_0 > 1$, the infected number of people are expected to increase, and for $\mathcal{R}_0 < 1$, transmissions are expected to fade or die out. The reproduction number is a central concept in infectious disease epidemiology, indicating the risk of an infectious agent with respect to epidemic spread. A valid estimation of the basic reproduction number $(\mathcal{R}_0)$ has the potential to help regarding prevention programs and intervention or mitigation strategies. The basic reproductive number $(\mathcal{R}_0)$ of COVID-19 has been initially estimated by WHO, CDC and other researchers to range between 2.0 and 4.0 (CDC, 2020; Liu et al., 2020; WHO, 2020; Zhao et al., 2020). This means each person with COVID-19 would on average, infect 2 to 4 other people in a totally susceptible population.

Using the next generation operator method described in (Diekmann et al., 2012; Driessche & Watmough, 2002; Heesterbeek, 2002), we establish the local stability of $\varkappa_o$. By model (1), we have

$$\frac{d}{dt}\begin{bmatrix} E_l \\ I_l \\ E_h \\ I_h \\ H \end{bmatrix} = \begin{bmatrix} \beta_l(1-\epsilon_l)(I_h + I_l + \nu H)\dfrac{S_l}{N} \\ 0 \\ \beta_h(1-\epsilon_h)(I_l + I_h + \nu H)\dfrac{S_h}{N} \\ 0 \\ 0 \end{bmatrix} - \begin{bmatrix} k_l E_l \\ (\sigma_l + \delta_l)I_l - k_l E_l \\ k_h E_h \\ (\sigma_h + \delta_h)I_h - k_h E_h \\ \alpha H - (\rho_h \sigma_h I_h + \sigma_l \rho_l I_l) \end{bmatrix},$$

from which the matrix F of new infection terms and matrix V of the transition terms are given by

$$F = \begin{bmatrix} 0 & \beta_l(1-\epsilon_l)\dfrac{S_l(0)}{N(0)} & 0 & \beta_l(1-\epsilon_l)\dfrac{S_l(0)}{N(0)} & \beta_l(1-\epsilon_l)\nu\dfrac{S_l(0)}{N(0)} \\ 0 & 0 & 0 & 0 & 0 \\ 0 & \beta_h(1-\epsilon_h)\dfrac{S_h(0)}{N(0)} & 0 & \beta_h(1-\epsilon_h)\dfrac{S_h(0)}{N(0)} & \beta_h(1-\epsilon_h)\nu\dfrac{S_h(0)}{N(0)} \\ 0 & 0 & 0 & 0 & 0 \\ 0 & 0 & 0 & 0 & 0 \end{bmatrix}$$

and,

$$V = \begin{bmatrix} k_l & 0 & 0 & 0 & 0 \\ -k_l & \sigma_l + \delta_l & 0 & 0 & 0 \\ 0 & 0 & k_h & 0 & 0 \\ 0 & 0 & -k_h & \sigma_h + \delta_h & 0 \\ 0 & -\sigma_l \rho_l & 0 & -\sigma_l \rho_l & \alpha \end{bmatrix}.$$

The effective reproduction number $(\mathcal{R}_0)$ of the model (1) is the spectral radius of the product FV^{-1} and it is given by

$$\mathcal{R}_0 = \mathcal{R}_l + \mathcal{R}_h = \frac{(1-\epsilon_l)\beta_l(\alpha + \nu\sigma_l\rho_l)S_l(0)}{N(0)\alpha(\sigma_l + \delta_l)} + \frac{(1-\epsilon_h)\beta_h(\alpha + \nu\sigma_h\rho_h)S_h(0)}{N(0)\alpha(\sigma_h + \delta_h)}$$

4. Results and discussion

This section narrates the findings and discusses the various results of the analyses performed on our proposed model. The proposed model was calibrated to Brazil and South Africa COVID-19 cumulative data (Johns Hopkins University., 2020). Twelve parameters were used to enable us to determine the inexact of the model and to obtain better graphical and table representations.

4.1. Fitted parameters of the model

We constructed a deterministic population-based compartmental model of COVID-19 transmission with intervention measures. Data for the model were obtained from the Center for Systems Science and Engineering (CSSE) at Johns Hopkins University (JHU) of Coronavirus COVID-19 Global Cases team (Johns Hopkins University., 2020). To validate our proposed model, we used Brazil and South Africa as our case study. The rationale for using these two countries was purely based on their geographical location and the increasing number of infected cases of COVID-19 in South America and Africa in general. We chose March 3, 2020, as a starting point because the first week of March 2020 was when the first official COVID-19 cases were reported in both countries.

Around the first week of March 2020, the total population in Brazil was 212,615,886. Around the same time in March 2020, one individual was infected with COVID-19, and these cases represented the initial infected $I_l(0)$ compartment. We assumed that 2100 were initial exposed $E_l(0)$ compartment; we further assumed that 30% of the total population were high-risk of the susceptible compartment. Those initially exposed in high risk $E_h(0)$ compartment were about 200. However, initial infected $I_h(0)$ in high risk, hospitalization $H(0)$ and recovery $R(0)$ compartment were zero (0).

Similarly, about the first week in March 2020, the total population in South Africa was 59,334,579. About the same time in March 2020, one individual was infected with COVID-19, and these cases represented the initial infected $I_l(0)$ compartment. We assumed that 250 individuals were initially exposed $E_l(0)$; we further assumed that 30% of the total population are high-risked. Those initially exposed in high risk $E_h(0)$ compartment were about 30. But, initial infected $I_h(0)$ in high risk, hospitalization $H(0)$ and recovery $R(0)$ compartment were zero (0).

Using the *fmincon* Optimization Toolbox incorporated in MATLAB, the data fitting method entails applying the traditional nonlinear least-squares approach. The data plots and the best-fit model for daily reported cumulative cases of COVI-19 in Fig. 2 and 3, represent Brazil and South Africa, respectively. The observed daily cumulative data points are displayed in the red dot, and the blue curve represents the best-fitting curve for the proposed model. The estimated parameter values are reported in Table 4 and were used for prediction in the graphs in section 4.3. The estimated parameter values were also used to compute the value for $\mathcal{R}_l$, $\mathcal{R}_h$, and the overall $\mathcal{R}_0$ for the model in Table 4.

4.2. Analysis of the effective reproduction number

In this section, we present the contour plots of effective reproduction number with respect to ϵ_l against ϵ_h. The contour plots of $\mathcal{R}_0$ for the two countries are discussed below.

Fig. 4 displays a contour plot of the effective reproduction number as a function of non-pharmaceutical interventions by both risk subpopulations in Brazil. The result in Fig. 4 shows that if transmission can be reduced by at least 20% by the high-risk population and about 50% by the low-risk population, the effective reproduction number will fall below one, and the spread of the virus will fade out. If $\epsilon_h = 0$, then at least 56% reduction of transmission rate by the low-risk population was needed to eliminate the disease. Fig. 4 also suggests that, with almost no interventions by both risk subpopulation, the basic or effective reproduction will stay around 1.76, indicating that an infectious individual will be capable of passing the virus to, on average, 1.76 susceptible individuals.

Similarly, the findings for South Africa in Fig. 5 warrant at least a 20% reduction in the transmission rate by the high-risk population and approximately 70% reduction in the low-risk population to decrease the effective reproduction number below one, and ultimately the spread of the virus will decrease or dissipate. Contrarily, the virus will continue to spread. The contour plot in Fig. 5 implies that, with nearly no interventions or precautions taken by both risk (low and high) subpopulation groups, the basic or effective reproduction number will stay above 2. This means that an infected individual would, on average, be able to spread the virus to at least 2 vulnerable persons.

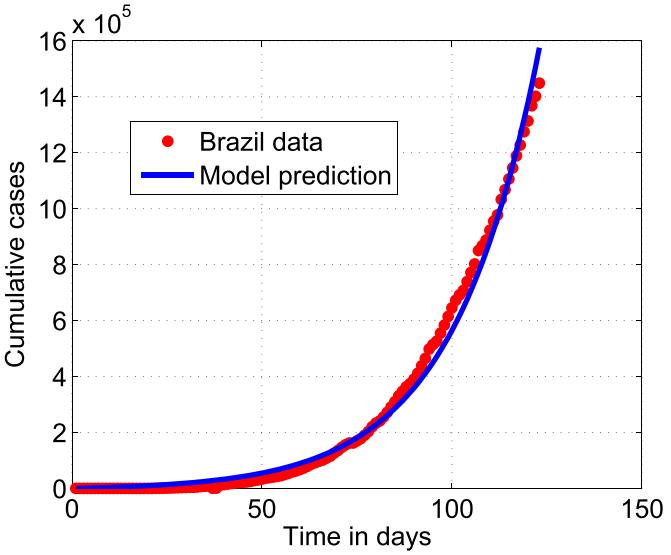

Fig. 2. Fitting plot, Brazil.

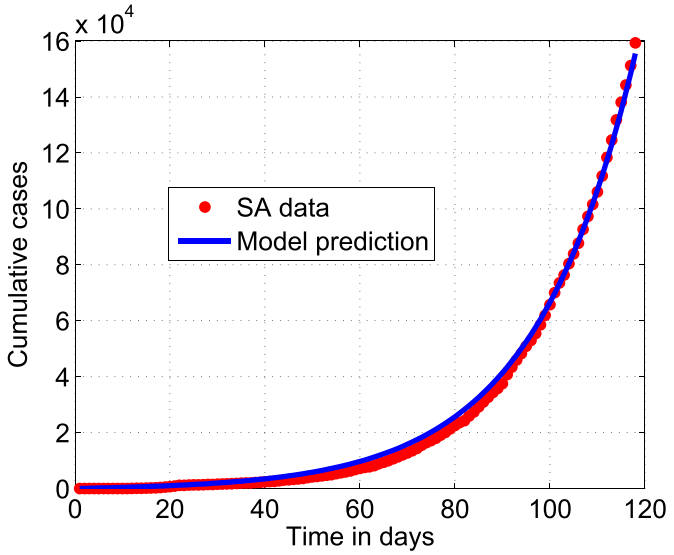

Fig. 3. Fitting plot, South Africa.

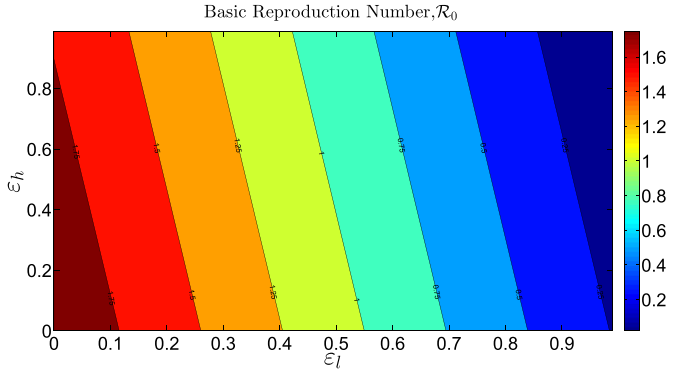

Fig. 4. Contour plot, Brazil.

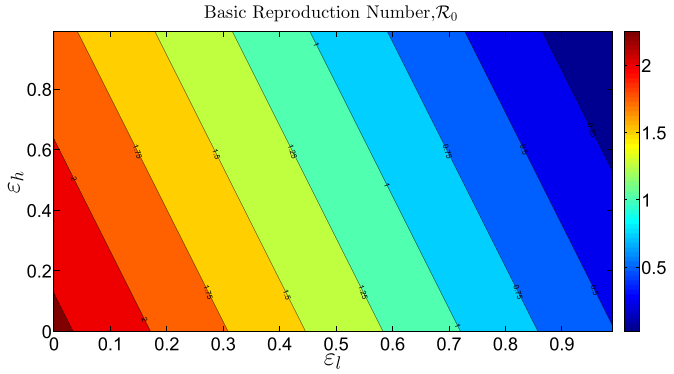

Fig. 5. Contour plot, South Africa.

4.3. *Effects of* ϵ_l

This section analyzes the effects of ϵ_l on susceptible and infective populations for Brazil and South Africa. The area under the curves measures the population of individuals over the given interval.

4.3.1. Case 1: Brazil

In this subsection, we examined the effect of non-pharmaceutical intervention by low-risk to prevent the acquisition of infection by susceptible individuals on susceptible low-risk, infected low-risk, susceptible high-risk, and infected high-risk for Brazil. These effects are shown in Figs. 6–9 respectively. Fig. 6 shows the effects of ϵ_l on susceptible low-risk population. Increasing ϵ_l increases the susceptible low-risk population. Similarly, we noted that the same trend is observed in Fig. 8. In Figs. 7–8, we observed that increasing non-pharmaceutical intervention reduces the infectious population for both low-risk and high-risk populations. We also observed that Brazil peaked between ninety days and one hundred and eighty days, corresponding to the least non-pharmaceutical intervention and the highest non-pharmaceutical intervention, respectively.

As shown in Table 5, a decrease in the non-pharmaceutical intervention (baseline) increases the infected cases in both low-risk and high-risk populations. Whereas increasing the baseline decreases the infected cases in both low-risk and high-risk

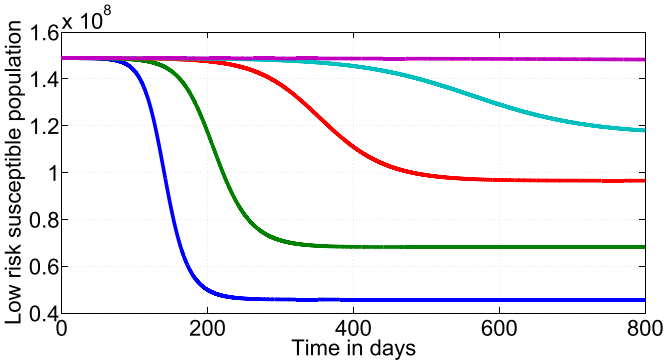

Fig. 6. Impact of ϵ_l on S_l, Brazil.

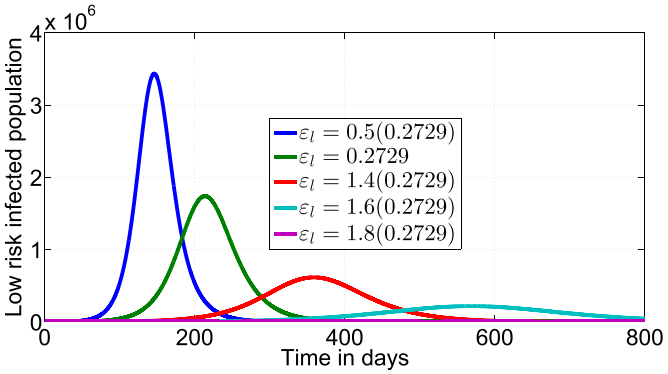

Fig. 7. Impact of ϵ_l on I_l, Brazil.

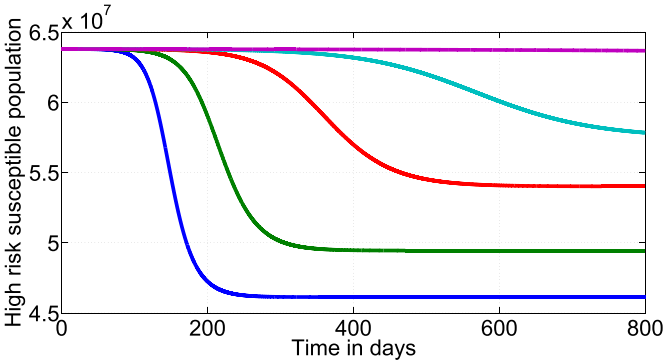

Fig. 8. Impact of ϵ_l on S_h, Brazil.

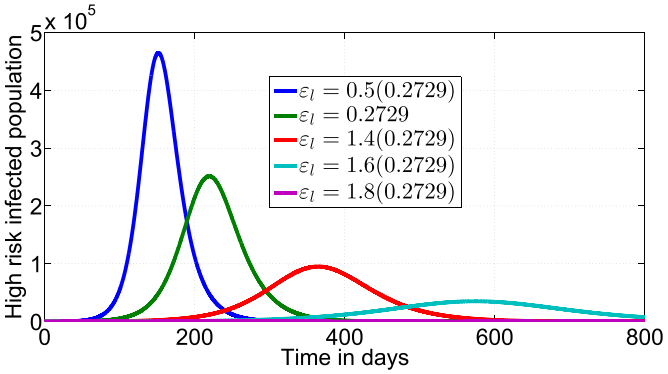

Fig. 9. Impact of ϵ_l on I_h, Brazil.

Table 5
Effect of ϵ_l on the infected subpopulations in Brazil on the interval [0,800]. These estimates represent the cumulative cases over the given time interval.

Changes in ϵ_l	Low-risk infected pop.	High-risk infected pop.
Baseline	$1.692\ 8 \times 10^8$	$2.508\ 8 \times 10^7$
50% reduction of the baseline	$2.163\ 1 \times 10^8$	$3.087\ 4 \times 10^7$
40% increase in the baseline	$1.098\ 0 \times 10^8$	$1.709\ 0 \times 10^7$
60% increase in the baseline	$6.457\ 4 \times 10^7$	$1.036\ 8 \times 10^7$
80% increase in the baseline	$1.222\ 3 \times 10^6$	$2.035\ 7 \times 10^5$

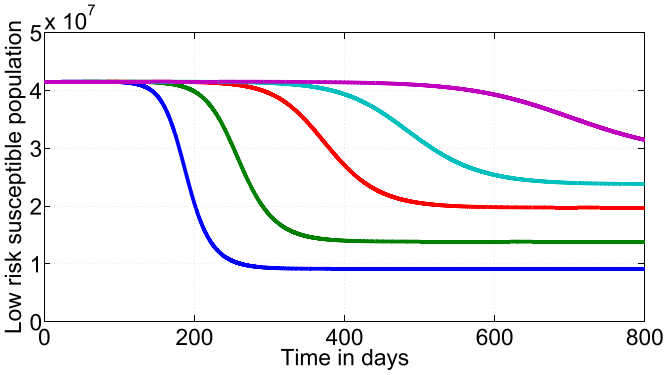

Fig. 10. Impact of ϵ_l on S_l, South Africa.

populations. This behaviour implies that: a) the higher the increase in the baseline, the lower the spread of the disease in both populations, and b) the faster the spread of the disease, the lower the level in the baseline.

4.3.2. Case 2: South Africa

In this subsection, we studied the effect of non-pharmaceutical intervention by low-risk to prevent the acquisition of infection by susceptible individuals on susceptible low-risk, infected low-risk, susceptible high-risk and infected high-risk for South Africa. These effects are shown in Figs. 10–13 respectively. Fig. 10 shows the effect of ϵ_l on susceptible low-risk population. Increasing ϵ_l increases the susceptible low-risk population. Similarly, we noted that the same trend is observed in Fig. 12. In Figs. 11–12, we observed that increasing non-pharmaceutical intervention reduces the infectious population for both low-risk and high-risk populations. We also observed South Africa reaching a peak between one hundred and two hundred days corresponding to the least non-pharmaceutical intervention and the highest non-pharmaceutical intervention.

As shown in Table 6, decreasing in the non-pharmaceutical intervention (baseline) increases the infected cases in both low-risk and high-risk populations. Whereas increasing the baseline decreases the infected cases in both low-risk and high-risk populations. This behaviour implies that: a) Increasing non-pharmaceutical interventions may allow the South African government to adequately prepare its health resources, and b) the quicker the disease progresses, the baseline level becomes lower.

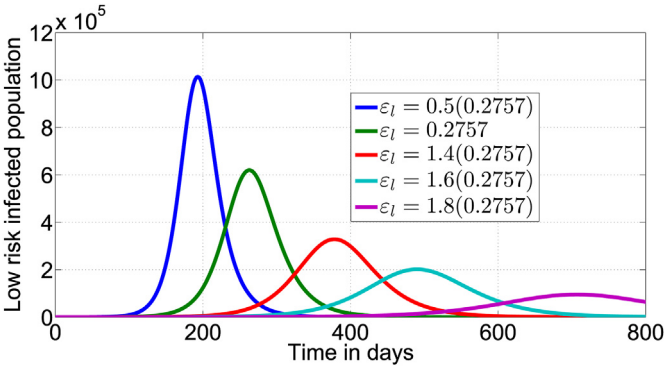

Fig. 11. Impact of ϵ_l on I_l, South Africa.

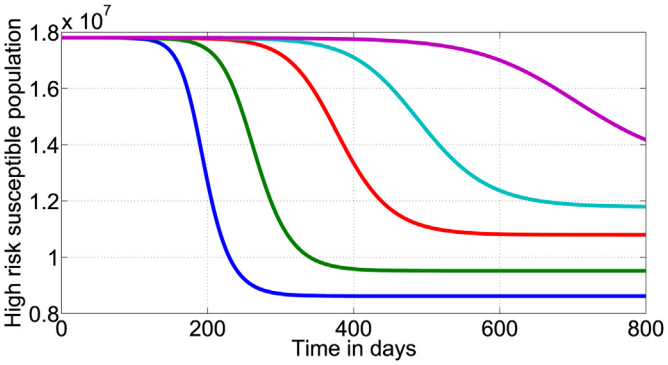

Fig. 12. Impact of ϵ_l on S_h, South Africa.

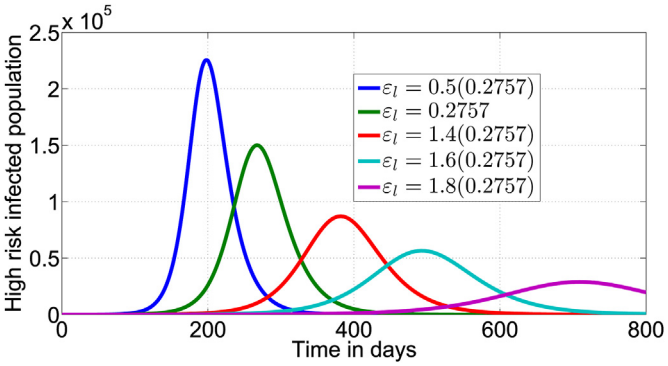

Fig. 13. Impact of ϵ_l on I_h, South Africa.

Table 6
Effect of ϵ_l on the infected subpopulations in South Africa on the interval [0,800].

Changes in ϵ_l	Low-risk infected pop.	High-risk infected pop.
Baseline	$5.811\,5 \times 10^7$	1.45×10^7
50% reduction of the baseline	$6.799\,4 \times 10^7$	$1.606\,6 \times 10^7$
40% increase in the baseline	$4.573\,9 \times 10^7$	$1.226\,3 \times 10^7$
60% increase in the baseline	$3.718\,5 \times 10^7$	$1.049\,9 \times 10^7$
80% increase in the baseline	$2.075\,6 \times 10^7$	$6.233\,6 \times 10^6$

4.4. Effects of ϵ_h

This section examines the effects of ϵ_h, which are precautions taken by high-risk individuals on susceptible and infectious populations for Brazil and South Africa. These precautions include staying at home and avoiding crowded gatherings, minimizing visiting shopping places, wearing masks at all times when outside, and washing hands with soap regularly and consistently.

4.4.1. Case 1: Brazil

The effect of ϵ_h on the various populations were examined in this subsection. Figs. 14-17 show the effect of ϵ_h on the low-risk susceptible populations and the high-risk susceptible populations respectively. We observed that increasing the non-pharmaceutical intervention by high-risk to prevent infection does not substantially impact the low-risk susceptible population dynamics. Still, it greatly impacts the high-risk susceptible population, as shown in Fig. 16. A similar trend is observed in the infectious populations. Increasing ϵ_h results in a decrease in both subgroup infectious populations but more pronounced in the high-risk populations, and a smaller impact on the low-risk infectious population. This indicates that high-risk individuals taking precautions result in a decrease in the infection rate in their subgroup but do not have a considerable effect on the low-risk infectious population. For example, in Table 7, a 50% reduction in the baseline of ϵ_h will result in about 1.791 4×10^8 of infections in the low-risk infected populations as compared to 3.299 8×10^7 found in the high-risk population. A similar trend was observed in both the low and high-risk populations when there was an increase in ϵ_h, as shown in Table 7. The infectious populations peaked around one hundred and twenty days from the first case reported for low-risk and high-risk populations. Hence the dynamics of ϵ_h largely impacted the high-risk susceptible and infectious populations.

4.4.2. Case 2: South Africa

Again, in this subsection, we studied the effect of ϵ_h on the South African subgroup populations. Figs. 18-21 show the effects of ϵ_h on the low-risk susceptible populations and the high-risk susceptible populations respectively. We observed that increasing the non-pharmaceutical intervention by high-risk to prevent infection does not significantly impact the dynamics of the low-risk susceptible population, but it greatly impacted the high-risk susceptible population, as shown in Fig. 20. A similar trend was observed with the infectious populations. Increasing ϵ_h caused a reduction in both subgroup infectious populations but with a higher decrease in the high-risk population and a lesser impact on the low-risk infectious populations.

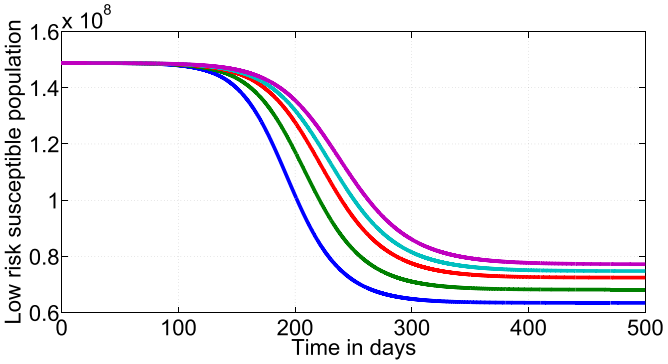

Fig. 14. Impact of ϵ_h on S_l, Brazil.

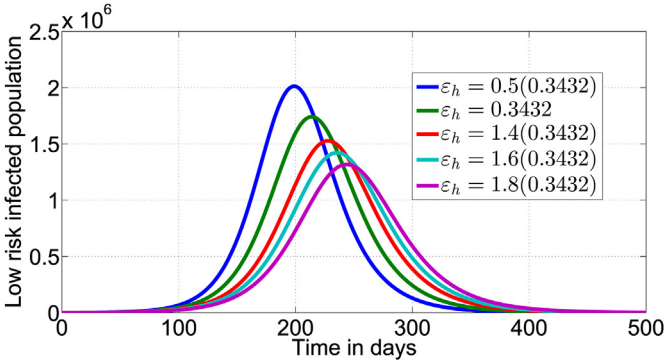

Fig. 15. Impact of ϵ_h on I_l, Brazil.

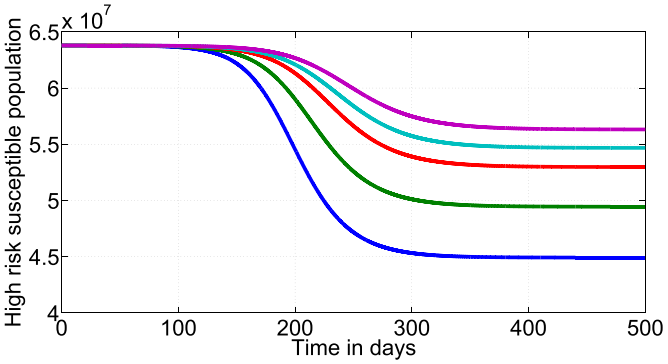

Fig. 16. Impact of ϵ_h on S_h, Brazil.

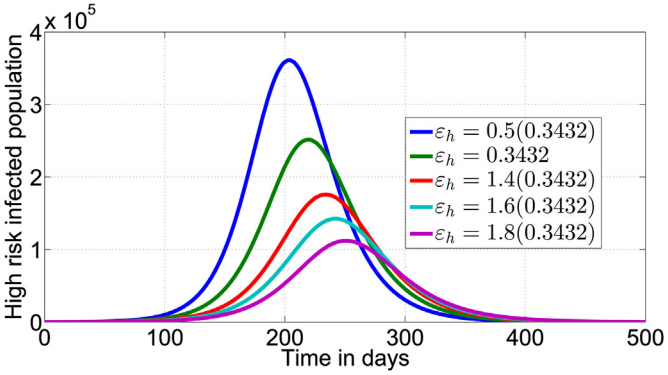

Fig. 17. Impact of ϵ_h on I_h, Brazil.

Table 7
Effect of ϵ_h on the infected subpopulations in Brazil on the interval [0,500].

Changes in ϵ_h	Low-risk infected pop.	High-risk infected pop.
Baseline	$1.692\ 7 \times 10^8$	$2.508\ 6 \times 10^7$
50% reduction of the baseline	$1.791\ 4 \times 10^8$	$3.299\ 8 \times 10^7$
40% increase in the baseline	$1.602\ 6 \times 10^8$	$1.891\ 0 \times 10^7$
60% increase in the baseline	$1.553\ 8 \times 10^8$	$1.593\ 4 \times 10^7$
80% increase in the baseline	$1.502\ 4 \times 10^8$	$1.306\ 2 \times 10^7$

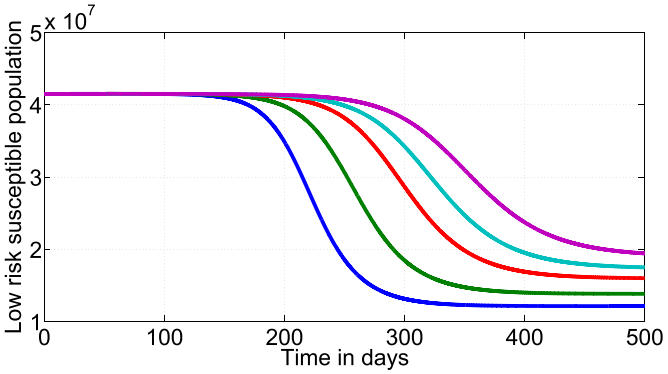

Fig. 18. Impact of ϵ_h on S_l, South Africa.

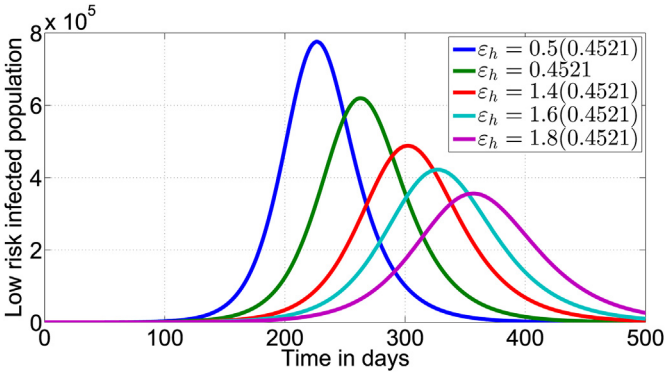

Fig. 19. Impact of ϵ_h on I_l, South Africa.

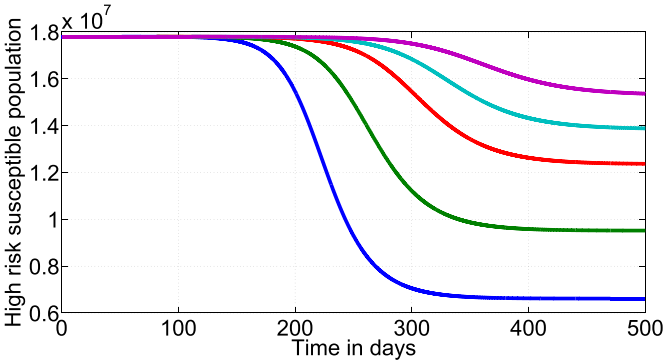

Fig. 20. Impact of ϵ_h on S_h, South Africa.

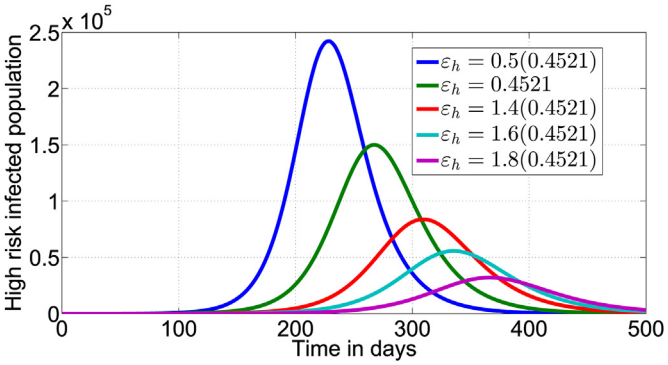

Fig. 21. Impact of ϵ_h on I_h, South Africa.

For example, in Table 8, a 50% reduction in the baseline of ϵ_h will result in about 5.809 8 $\times$ 10^7 of infections in the low-risk infected population as compared to 1.957 6 $\times$ 10^7 found in the high-risk population. A similar trend was observed in both the low and high-risk populations when there was an increase in ϵ_h, as shown in Table 8. The infectious populations peaked around one hundred and fifty days from the first case reported for both low-risk and high-risk populations. Hence the dynamics of ϵ_h greatly impacted the high-risk susceptible and infectious populations.

4.5. Comparing the two measures: ϵ_l vs. ϵ_h

In addition to the above observations about the effects of low and high-risk individuals' preventive actions, we directly compared the two measures. Firstly, we computed the sensitivity indices of the effective reproduction number, $\mathcal{R}_0$, in terms of the two measures. The index measures the relative change in $\mathcal{R}_0$ with respect to the relative change in ϵ_l or ϵ_h (Apenteng,

Table 8
Effect of ϵ_h on the infected subpopulations in South Africa on the interval [0,500].

Changes in ϵ_h	Low risk-infected pop.	High-risk infected pop.
Baseline	$6.167\,5 \times 10^7$	$1.449\,5 \times 10^7$
50% reduction of the baseline	$5.809\,8 \times 10^7$	$1.957\,6 \times 10^7$
40% increase in the baseline	$5.353\,0 \times 10^7$	$9.498\,4 \times 10^6$
60% increase in the baseline	$5.035\,7 \times 10^7$	$6.847\,0 \times 10^6$
80% increase in the baseline	$4.621\,1 \times 10^7$	$4.243\,1 \times 10^6$

Oduro, & Owusu-Mensah, 2021; Nakul, Hyman, & Cushing, 2008; Oduro et al., 2020; Rosa and Torres, 2018). To determine the relative impact of each parameter on the transmission of the disease, sensitivity analysis was important.

Definition: The normalized forward sensitivity index of a variable, L, that depends differentially on a parameter, y, is defined as:

$$\Phi_y = \frac{y}{L}\frac{\partial L}{\partial y}.$$

The sensitivity indices of $\mathcal{R}_0$ for the two measures are computed below.

$$\begin{aligned}\Phi_{\epsilon_l} &= \frac{\partial \mathcal{R}_0}{\partial \epsilon_l}\frac{\epsilon_l}{\mathcal{R}_0} = \frac{-\beta_l(\alpha+\nu\sigma_l\rho_l)S_l(0)}{N(0)\alpha(\sigma_l+\delta_l)}\frac{\epsilon_l}{\mathcal{R}_0}\\ \Phi_{\epsilon_h} &= \frac{\partial \mathcal{R}_0}{\partial \epsilon_h}\frac{\epsilon_h}{\mathcal{R}_0} = \frac{-\beta_h(\alpha+\nu\sigma_h\rho_h)S_h(0)}{N(0)\alpha(\sigma_h+\delta_h)}\frac{\epsilon_h}{\mathcal{R}_0}\end{aligned} \tag{3}$$

Using equation (3) and the values of parameters in Tables 3 and 4 for Brazil, we obtain $\Phi_{\epsilon_l} = -0.336\,2$ and $\Phi_{\epsilon_l} = -0.054\,5$. Similarly, in South Africa, we have $\Phi_{\epsilon_l} = -0.316\,2$ and $\Phi_{\epsilon_l} = -0.139\,7$. Both preventive parameters reduce the effective reproduction number; the low-risk individuals' preventive actions are more sensitivity and impactive.

Next, we compared the quantitative reduction or rise of infected cases by varying the two measures simultaneously. The quantitative change was analyzed in terms of the time evolution of the infected populations on the period [0, 600] and [0, 800] for Brazil and South Africa, respectively. The values of parameters used were displayed in Tables 3 and 4 unless otherwise stated. The results for Brazil are shown in Fig. 22 and Table 9, and that of South Africa in Fig. 23 and Table 10. Below, the findings were further clarified.

(i) Scenario 1: We considered the baseline of ϵ_l and ϵ_h. As displayed in Fig. 22 and Table 9, about $1.692\,7 \times 10^8$ of the low-risk and $2.508\,6 \times 10^7$ of the high-risk individuals contract the infection during Brazil's study period. Fig. 22 and Table 10 show that, in South Africa, approximately $5.811\,4 \times 10^7$ of the low-risk and $1.450\,0 \times 10^7$ of the high-risk may acquire the virus.

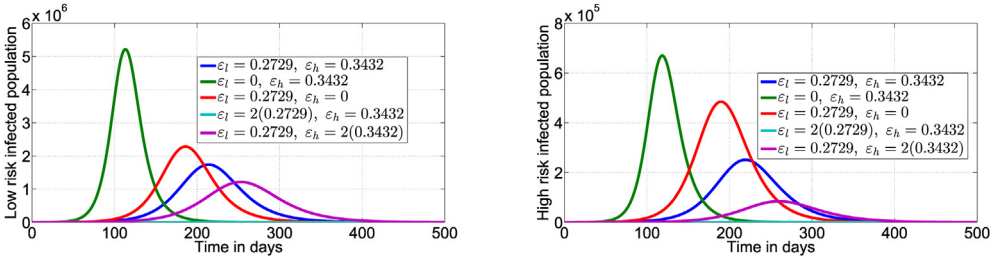

Fig. 22. Effects of ϵ_l *vs.* ϵ_h on I_h, Brazil.

Table 9
Quantitative effects of ϵ_l *vs.* ϵ_h in infected populations for Brazil on the interval [0,500].

Changes in ϵ_h	Low-risk infected pop.	High-risk infected pop.
$\epsilon_l = 0.272\,9$, $\epsilon_h = 0.343\,2$	$1.692\,7 \times 10^8$	$2.508\,6 \times 10^7$
$\epsilon_l = 0$, $\epsilon_h = 0.343\,2$	$2.459\,4 \times 10^8$	$3.429\,7 \times 10^7$
$\epsilon_l = 0.272\,9$, $\epsilon_h = 0$	$1.875\,7 \times 10^8$	$4.083\,8 \times 10^7$
$\epsilon_l = 2(0.272\,9)$, $\epsilon_h = 0.343\,2$	$5.621\,8 \times 10^4$	$1.001\,5 \times 10^4$
$\epsilon_l = 0.272\,9$, $\epsilon_h = 2(0.343\,2)$	$1.448\,3 \times 10^8$	$1.031\,9 \times 10^7$

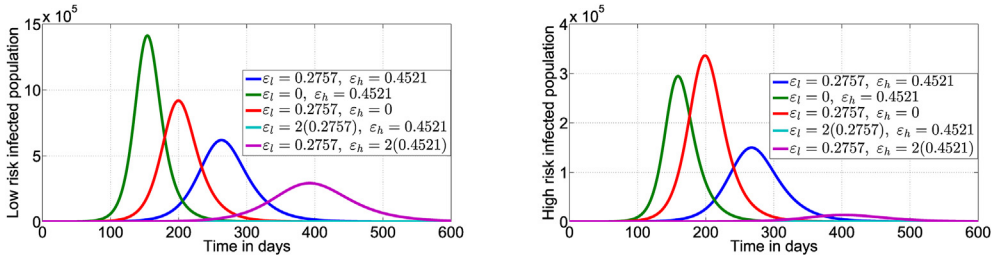

Fig. 23. Effects of ϵ_l *vs.* ϵ_h on I_h, South Africa.

Table 10
Quantitative effects of ϵ_l *vs.* ϵ_h in infected populations for South Africa on the interval [0,600].

Changes in ϵ_h	Low-risk infected pop.	High-risk infected pop.
$\epsilon_l = 0.275\ 7, \epsilon_h = 0.452\ 1$	$5.811\ 4 \times 10^7$	1.45×10^7
$\epsilon_l = 0, \epsilon_h = 0.452\ 1$	$7.419\ 9 \times 10^7$	$1.696\ 2 \times 10^7$
$\epsilon_l = 0.275\ 7, \epsilon_h = 0$	$6.382\ 4 \times 10^7$	$2.324\ 1 \times 10^7$
$\epsilon_l = 2(0.275\ 7), \epsilon_h = 0.452\ 1$	$8.117\ 8 \times 10^4$	$2.677\ 9 \times 10^4$
$\epsilon_l = 0.275\ 7, \epsilon_h = 2(0.452\ 1)$	$4.293\ 4 \times 10^7$	$2.037\ 4 \times 10^6$

(ii) Scenario 2: When $\epsilon_l = 0$ but $\epsilon_h = 0.343\ 2$, the total infected cases in Brazil for the low-risk population increase by about 45% compared to the observed cases in scenario 1. While infections in the high-risk population also rise by approximately 37%. In South Africa, when $\epsilon_l = 0$ but $\epsilon_h = 0.452\ 1$, the percentage changes, compared to the baseline cases, are about 28% and 17% increase for the low-and high risks populations, respectively.

(iii) Scenario 3: In Brazil, when $\epsilon_l = 0.272\ 9$ but $\epsilon_h = 0$, the percentage changes, compared to the baseline cases, are approximately 10% and 63% increase for the low-and high risks populations, respectively. While in South Africa, the percentage changes are 10% and 60% in the low and high-risk individuals, respectively.

(iv) Scenario 4: With a 100% increase in the estimated ϵ_l but an unchanged ϵ_h, almost 100% decrease in total infected cases in both risk populations would occur. This effect is observed in both Brazil and South Africa.

(v) Scenario 5: In Brazil, with a fixed baseline ϵ_l and a 100% increase in ϵ_h yields 14% and 59% reduction in the number of infected cases for the low and high-risk populations respectively. The reductions in South Africa for low and high-risk individuals are 26% and 86%, respectively.

These findings indicate that the mitigation efforts of low-risk individuals may be preferred to the efforts of high-risk individuals because they have a higher impact on the incidence of infection in low-risk and high-risk populations.

5. Summary and recommendations

The spread and severity of the novel coronavirus disease (COVID-19), has become an unprecedented threat to public health worldwide. For several years, researchers have used different scientific tools to provide deeper insights into disease models' dynamics and predicted the spread of diseases. As of writing this article, there was no vaccine or cure, besides human behavioral measures including face mask, social distancing, isolating, and washing of hands regularly with soap. It is essential to predict the development trend of the epidemic effectively, including peaking time and peaking value. It is also equally necessary to assess the impact of non-pharmaceutical measures. In this article, we presented a COVID-19 mathematical model of at-risk populations with non-pharmaceutical preventive measures. In particular, we incorporated two preventive measures, such as non-pharmaceutical strategies by both low and high-risk individuals, to reduce infection transmission. Our goal was to evaluate the role of these measures on the transmission of the disease and ultimately provide recommendations that may be useful to the general public. The proposed model was fitted to data from Brazil and South Africa.

Based on the estimated model parameters, we computed the effective reproduction numbers for both risk populations and the overall population, as shown in Table 4. The results obtained in Table 4 suggest that the $\mathcal{R}_h$ in each country under study had lower values. This could be attributed to the effect of the extra precautions by the high-risk populations. Additionally, the overall $\mathcal{R}_0$, as displayed in Table 4, suggests that the infection spreads slightly higher in South Africa than Brazil, in the period of study. We further analyzed the effective reproduction numbers using contour plots. The results from the contour plots showed that, in Brazil, at least a 20% reduction of transmission rate by the high-risk population and 50% reduction of transmission rate by the low-risk population would be required for the reproduction number to fall below one. Similarly, a minimum of 20% of compliance of ϵ_h will warrant at least 70% of ϵ_l in South Africa to drop the $\mathcal{R}_0$ below one. These results suggest that the baseline value for non-pharmaceutical intervention by the low-risk subpopulation is not enough to eliminate the spread of the disease.

Based on our numerical simulations and the findings, non-pharmaceutical interventions by high-risk individuals only significantly reduced infections among the high-risk individuals, but did not have a substantial impact on the low-risk population. In contrast, non-pharmaceutical interventions by low-risk individuals had a significant impact in both subgroups. Thus, the low-risk individuals' preventive actions significantly reduced infections, even among high-risk individuals. This observation could be explained by the high effective contact rate of the low-risk individuals.

Though the above results are based on non-pharmaceutical interventions, the study was conducted when there were no COVID-19 vaccines or drugs. However, the results can be applied to the ongoing COVID-19 vaccinations. That is, vaccination by the low-risk individuals has a high tendency to reduce the infection. We highly recommend that the low-risk individuals strongly comply with the non-pharmaceutical measures and also get vaccinated to protect themselves and the high-risk groups that are more susceptible or vulnerable to the infection. In addition, we encourage the general public to adhere to the COVID-19 protocols and get immunized with the vaccine.

Availability of data and materials

The data used in this paper is cited throughout the paper.

Declaration of competing interest

There is no competing interests.

Funding

No source of funding for this work.

Authors' contributions

All authors evenly contributed to the whole work. All authors read and approved the final manuscript.

Ethical approval

This article does not contain any studies with human participants performed by any of the authors.

Acknowledgments

Not applicable.

References

Anderson, R. M., Heesterbeek, H., Klinkenberg, D., & Hollingsworth, T. D. (2020). How will country-based mitigation measures influence the course of the COVID-19 epidemic? *The Lancet, 10228*(395), 931–934. Elsevier.

Apenteng, O. O., Oduro, B., & Owusu-Mensah, I. (2021). A compartmental model to investigate the dynamics of the COVID−19 pandemic: A case study in five countries. *International Journal of Biomathematics, 14*(05), Article 2150027. https://doi.org/10.1142/S1793524521500273

Bai, Y., Yao, L., Wei, T., Tian, F., Jin, D. Y., Chen, L., et al. (2020). Presumed asymptomatic carrier transmission of COVID-19. *Jama, 323*(14), 1406–1407.

Chen, T., Wu, D., Chen, H., Yan, W., Yang, D., Chen, G., et al. (2020). Clinical characteristics of 113 deceased patients with coronavirus disease 2019: Retrospective study. *BMJ, 368*.

Diekmann, O., Heesterbeek, J. A. P., & Britton, T. (2012). *Mathematical tools for understanding infectious disease dynamics* (Kindle Edition). Princeton University Press.

Driessche, P. V., & Watmough, J. (2002). Reproduction numbers and sub-threshold endemic equilibria for compartmental models of disease transmission. *Mathematical Biosciences, 180*, 29–48.

Ferguson, N. M., Laydon, D., Nedjati-Gilani, G., Imai, N., Ainslie, K., Baguelin, M., et al. (2020). *Impact of non-pharmaceutical interventions (NPIs) to reduce COVID19 mortality and healthcare demand*. London: Imperial College COVID-19 Response Team.

Guan, W. J., Ni, Z. Y., Hu, Y., Liang, W. H., Ou, C. Q., He, J. X., et al. (2020). Clinical characteristics of coronavirus disease 2019 in China. *New England Journal of Medicine, 382*(18), 1708–1720.

Heesterbeek, J. A. P. (2002). A brief history of *R*0 and a recipe for its calculation. *Acta Biotheoretica, 50*, 189–204.

Huang, C., Wang, Y., Li, X., Ren, L., Zhao, J., Hu, Y., et al. (2020). Clinical features of patients infected with 2019 novel coronavirus in Wuhan, China. *The Lancet, 395*(10223), 497–506.

Jewell, N. P., Lewnard, J. A., & Jewell, B. L. (2020). Predictive mathematical models of the COVID-19 pandemic: Underlying principles and value of projections. *Jama, 323*(19), 1893–1894.

Johns Hopkins University. (2020). *COVID-19 dashboard by the center for systems science and engineering (CSSE) at*. Johns Hopkins University (JHU). https://coronavirus.jhu.edu/map.html.

Kobayashi, T., Jung, S. M., Linton, N. M., Kinoshita, R., Hayashi, K., Miyama, T., et al. (2020). *Communicating the risk of death from novel coronavirus disease (COVID-19)*.

Li, Q., Guan, X., Wu, P., Wang, X., Zhou, L., Tong, Y., et al. (2020). Early transmission dynamics in Wuhan, China, of novel coronavirus–infected pneumonia. *New England Journal of Medicine, 382*(13), 1199–1207.

Martins-Chaves, R. R., Gomes, C. C., & Gomez, R. S. (2020). Immunocompromised patients and coronavirus disease 2019: A review and recommendations for dental health care. *Brazilian Oral Research, 34*.

Mishra, S., Fisman, D. N., & Boily, M. C. (2011). The ABC of terms used in mathematical models of infectious diseases. *Journal of Epidemiology & Community Health, 65*(1), 87–94.

Nakul, C., Hyman, J. M., & Cushing, J. M. (2008). Determining important parameters in the spread of malaria through the sensitivity analysis of a mathematical model. *Bulletin of Mathematical Biology, 70*, 1272–1296.
Ndairou, F., Area, I., Nieto, J. J., & Torres, D. F. (2020). *Mathematical modeling of COVID-19 transmission dynamics with a case study of Wuhan. Chaos*. Solitons & Fractals.
Ngonghala, C. N., et al. (2020). Mathematical assessment of the impact of non-pharmaceutical interventions on curtailing the 2019 novel Coronavirus. *Mathematical Biosciences, 325*, 108364. https://doi.org/10.1016/j.mbs.2020.108364
Oduro, B., Apenteng, O. O., & Nkansah, H. (2020). Assessing the effect of fungicide treatment on Cocoa black pod disease in Ghana: Insight from mathematical modeling. *Statistics, Optimization & Information Computing, 8*(2), 374–385.
Oduro, B., & Magagula, V. M. (2021). COVID-19 intervention models: An initial aggressive treatment strategy for controlling the infection. *Infectious Disease Modelling, 6*, 351–361.
Onder, G., Rezza, G., & Brusaferro, S. (2020). Case-fatality rate and characteristics of patients dying in relation to COVID-19 in Italy. *Jama, 323*(18), 1775–1776.
Rosa, S., & Torres, D. F. M. (2018). Parameter estimation, sensitivity analysis and optimal control of a periodic epidemic model with application to HRSV in Florida. *Statistics, Optimization & Information Computing, 6*, 139–149.
Tang, B., Wang, X., Li, Q., Bragazzi, N. L., Tang, S., Xiao, Y., et al. (2020). Estimation of the transmission risk of the 2019-nCoV and its implication for public health interventions. *Journal of Clinical Medicine, 9*, 462.
Wang, L., He, W., Yu, X., Hu, D., Bao, M., Liu, H., et al. (2020b). Coronavirus disease 2019 in elderly patients: Characteristics and prognostic factors based on 4-week follow-up. *Journal of Infection*.
Wang, C., Horby, P. W., Hayden, F. G., & Gao, G. F. (2020a). A novel coronavirus outbreak of global health concern. *The Lancet, 395*(10223), 470–473.
World Health Organization. (2020). *Coronavirus disease 2019 (COVID-19): Situation report* (Vol. 72).
Zheng, Y., Ma, Y., Zhang, J., et al. (2020). COVID-19 and the cardiovascular system. *Nature Reviews Cardiology, 17*, 259–260.
Zhou, F., Yu, T., Du, R., Fan, G., Liu, Y., Liu, Z., et al. (2020). Clinical course and risk factors for mortality of adult inpatients with COVID-19 in Wuhan, China: A retrospective cohort study. *The Lancet, 395*(10229), 1054–1062.
Zhu, N., Zhang, D., Wang, W., Li, X., Yang, B., Song, J., et al. (2020). A novel coronavirus from patients with pneumonia in China, 2019. *New England Journal of Medicine, 382*(8), 727–733.